4944–4954 *Nucleic Acids Research, 2009, Vol. 37, No. 15* *Published online 15 June 2009*
doi:10.1093/nar/gkp502

A novel nucleoid-associated protein of *Mycobacterium tuberculosis* is a sequence homolog of GroEL

Debashree Basu[1], Garima Khare[2], Shashi Singh[3], Anil Tyagi[2], Sanjeev Khosla[4] and Shekhar C. Mande[1,*]

[1]Laboratory of Structural Biology, Centre for DNA Fingerprinting and Diagnostics, Hyderabad 500001, [2]Department of Biochemistry, University of Delhi, South Campus, New Delhi 110021, [3]Centre for Cellular and Molecular Biology, Uppal Road, Hyderabad 500007 and [4]Laboratory of Mammalian Genetics, Centre for DNA Fingerprinting and Diagnostics, Hyderabad 500001, India

Received December 29, 2008; Revised May 18, 2009; Accepted May 22, 2009

ABSTRACT

The *Mycobacterium tuberculosis* genome sequence reveals remarkable absence of many nucleoid-associated proteins (NAPs), such as HNS, Hfq or DPS. In order to characterize the nucleoids of *M. tuberculosis*, we have attempted to identify NAPs, and report an interesting finding that a chaperonin-homolog, GroEL1, is nucleoid associated. We report that *M. tuberculosis* GroEL1 binds DNA with low specificity but high affinity, suggesting that it might have naturally evolved to bind DNA. We are able to demonstrate that GroEL1 can effectively function as a DNA-protecting agent against DNase I or hydroxyl-radicals. Moreover, Atomic Force Microscopic studies reveal that GroEL1 can condense a large DNA into a compact structure. We also provide *in vivo* evidences that include presence of GroEL1 in purified nucleoids, *in vivo* crosslinking followed by Southern hybridizations and immunofluorescence imaging in *M. tuberculosis* confirming that GroEL1: DNA interactions occur in natural biological settings. These findings therefore reveal that *M. tuberculosis* GroEL1 has evolved to be associated with nucleoids.

INTRODUCTION

Bacterial chromosomes are typically packaged into compact structures, termed nucleoids. The structure and dynamics of nucleoids is determined by several factors like DNA supercoiling, macromolecular crowding and architectural nucleoid-associated proteins (NAP). The NAP not only influence the structure of the chromosomes but are also involved in replication, recombination, repair and transcription (1,2). The protein composition of bacterial nucleoids varies with cell growth conditions and the growth phase (2,3). Due to their role in chromosome compaction, NAPs also affect basic regulatory processes such as transcription. The study of relative interplay of NAPs in nucleoid compaction and their role in global regulation of bacterial transcription is, however, an underexplored area.

More than 12 DNA-binding proteins have been identified in *Escherichia coli*, that participate in nucleoid formation (1,2). Among the most important members of bacterial nucleoids are HNS (Histone like nucleoid-structuring protein), HU (Histone like protein first isolated from Ribonuclease negative *E. coli* U93 strain), IHF (Integrative host factor) and Fis (Factor for inversion stimulation) (4,5). Various studies carried out on these proteins have revealed that the DNA-binding affinity of HNS depends on DNA curvature with a distinct preference for A/T rich tracts (6,7). HNS is also a global transcriptional regulator and silences genes involved in virulence and stress response (8–10). HU is a non specific DNA-binding protein, involved in DNA bending, supercoiling and compaction. It binds nicked, gapped, cruciform as well as single-stranded DNA (11,12) and is also involved in replication, recombination and repair (13). HU has also been proposed to counteract the effects of HNS (14). IHF is a sequence homolog of HU, but binds DNA in a sequence specific manner unlike HU. Fis, like HU and IHF can bend DNA upon binding with high affinity (6). The other prominent NAPs are Lrp (leucine-responsive protein), global-transcriptional repressors, CbpA and CbpB (curved DNA-binding protein), StpA, Dps and Hfq (1,2). Apart from the architectural proteins,

*To whom correspondence should be addressed. Tel: +91 40 24749401; Fax: +91 40 27155610; Email: shekhar@cdfd.org.in

DNA polymerase, RNA polymerase, recombination and repair enzymes and several transcription factors also associate with nucleoids in a temporal manner (2). The presence of several NAPs and their antagonistic functions depict heterogeneity and the global regulation of the balance of forces in bacterial nucleoids (6).

Mycobacterium tuberculosis (Mtb) genome sequence shows remarkable absence of many NAPs. In order to characterize proteins associated with nucleoids in Mtb, we have purified some of them and interestingly discovered that a novel NAP in Mtb is a sequence homolog of the GroEL chaperonin. We had earlier reported that Mtb GroELs are unable to form canonical tetradecamers, and thus are deficient in folding model substrates *in vitro* (15). Furthermore, one of the copies of the *groEL* genes in Mtb was seen to be undergoing rapid divergence, leading to the speculation that it might be acquiring a new biochemical or physiological function (16). We report here that Mtb GroEL1 is capable of recognizing nucleic-acid substrates, without sequence specificity, and plays a role in the condensation of DNA in nucleoid formation. We therefore hypothesize that gene duplication in *Mycobacterial groEL* genes might have led to the new biochemical property of GroEL molecules as a result of alterations in the oligomerization of the molecules.

MATERIALS AND METHODS

Purification of GroEL1 (Rv3417c)

GroEL1 without $(His)_6$ tag was previously cloned in our laboratory in the expression vector pKK233-2 and designated pKKGL1 (data not shown). Cell lysates overexpressing GroEL1 from this plasmid were subjected to precipitation with 30% Ammonium Sulphate. The pellet containing GroEL1 was dialyzed against 50 mM Tris–HCl pH 8.0 supplemented with 1 mM EDTA. The dialyzed protein was loaded on the anion exchanger, Q-Sepharose, and was washed with 50 mM Tris–HCl, pH 8.0, supplemented with 150 mM NaCl and 1 mM EDTA. Elution was achieved by increasing the salt concentration to 300 mM. Further purification was performed by Size Exclusion Chromatography (SEC) on the Superdex 200 HR 10/30 column (GE Healthcare). GroEL1 eluted out as a dimer in the SEC.

Biotin streptavidin pull-down purification

The biotinylated 5′ oligonucleotide, ACGGAGGGGCA TGACCCGGTGCGGGGCTTCTTGCACTCGGCATA GGCGAGTGCTAAGAATAACGTT (containing the CIRCE4FR element sequence), was annealed with the corresponding antisense oligonucleotide in order to form a dsDNA probe. The oligos were annealed by heating equimolar amounts in 0.5× TE (5 mM Tris–HCl pH 8.0, 0.5 mM EDTA, pH 8.0) to 95°C for 5 min and gradually cooling down to room temperature. Biotinylated oligos were coupled to the streptavidin beads (Streptavidin MagneSphere Paramagnetic particles, Promega) by incubating the biotinylated oligos and streptavidin coated beads in 5 mM Tris–HCl (pH 8.0), 0.5 mM EDTA and 500 mM NaCl for 15 min. The cell lysate in buffer (50 mM Tris–HCl pH 8.0, 30 mM NaCl) was allowed to bind to the beads for 1 h at 30°C with slight stirring and washed three times with wash buffer (50 mM Tris–HCl pH 8.0, 100 mM NaCl). The protein was eluted with a buffer containing 1M NaCl supplemented with 50 mM Tris–HCl pH 8.0.

Electrophoretic mobility shift assay (EMSA)

EMSA were used to study the binding of Mtb GroEL1 to different annealed and γ-P^{32} ATP end-labeled oligonucleotide DNA. DNA was incubated with protein in binding buffer A (10 mM HEPES pH 7.9, 10% Glycerol, 0.1 mM EDTA, 0.2 mM spermidine, 1 μg poly (dI/dC), 10 mM $MgCl_2$, 2 mM DTT) on ice for 1 h. The DNA-protein complexes were fractionated on a native polyacryamide gel in 0.25× TBE (22.25 mM Tris/Borate/0.25 mM EDTA), at 150 V, 4°C for 2–3 h. When noted, non $(His)_6$-tagged Mtb GroEL1, $(His)_6$-tagged Mtb GroEL1, Mtb GroEL2, *E. coli* GroEL, Human Hsp60, *M. leprae* Cpn60.2 were added at indicated amounts to the ^{32}P-labeled probe.

The different structured oligonucleotides were obtained by first labeling DNA and subsequent annealing and purification. The region of 100–240-bp upstream of *groES* (*Rv3418c*) was PCR amplified using primer 5′-TATA TATCTAGAGACACGCTGGCAACCAGGAA-3′ and 5′-TATATAGTCGACCCAGGTGATTCGGCATTCGT CC-3′, end-labeled and resolved on a 5% native PAGE at 150 V, 4°C. Although the binding buffers contained no monovalent salts, the protein and the oligonucleotides were suspended in buffers containing 150 mM NaCl and 500 mM NaCl respectively prior to these experiments, thus making 20 mM final concentration of NaCl during the EMSA experiments. Similar experiments were also carried out in the binding buffer with 200 mM NaCl. The gels were dried and analyzed by Typhoon Variable Mode Imager and Image Quant software.

RNA-binding assay

The binding of GroEL1 to RNA was studied by EMSA. The RNA (UUCUUGCACUCGGCAUAGGCGAGUG CUA) used in the assay was chemically synthesized (MWG Biotech) and γP^{32} ATP end-labeled. A quantity of 4 nM RNA was incubated with increasing concentration of protein in binding buffer (10 mM HEPES pH 7.9, 10% Glycerol, 0.1 mM EDTA, 0.2 mM spermidine, 1 μg poly (dI/dC), 10 mM $MgCl_2$, 2 mM DTT). The RNA–protein complexes were fractionated on a native polyacrylamide gel in 0.25× TBE at 150 V, 4°C for 2–3 h. All the buffers used in the RNA assay were prepared in DEPC treated water.

DNA major groove and minor groove-binding assay

To determine the major and minor groove-binding activities of Mtb GroEL1 to DNA, 4 nM of ^{32}P-labeled CIRCE2FR probe was pre-incubated with increasing concentrations of Actinomycin D (Gibco Biosciences) and Methyl green (Sigma) for 20 min at 30°C in a reaction volume of 20 μl in buffer A. Mtb GroEL1 (1 μM) was added to the reaction, and the incubation further

continued on ice for 1 h. The DNA–protein complexes thus obtained were resolved in a 7% polyacrylamide gel for 2 h at 150 V at 4°C.

DNA super coiling-protection assay

To demonstrate the ability of the protein to protect supercoiled DNA, 200 ng pBSK plasmid DNA was incubated with 14 μM of Mtb GroEL1 along with 0.4 μM $FeCl_3$, 10 mM DTT, 100 mM ethanol and 2 mM H_2O_2 in a reaction volume of 15 μl for 30 min at 37°C. The reaction was terminated by the addition of 10 mM EDTA, followed by phenol extraction of the sample and analyzing on a 1% agarose gel in 1× TAE at 100 V for 30 min at room temperature.

DNA-protection assay

DNA-protection assay was performed as described previously (17), with minor modifications. An amount of 7 μM Mtb GroEL1 was allowed to interact with linear DNA (2 μg of pBSK, 2958 bp linearized with EcoRI) for 1 h at 37°C in 10 mM NaCl, 0.5 mM EDTA, 10 mM Tris–HCl pH 8.0. Following incubation, the complex was treated with 1 U of DNase I (NEB) for 5 min at 37°C. Reactions were terminated by incubation at 75°C for 10 min, followed by treatment with proteinase K (50 μg), 5 mM $MgCl_2$, 2% SDS and 0.3 M sodium acetate for 1 h at 37°C. The protein was extracted with phenol; DNA was precipitated with ethanol and 5 μg of glycogen, and loaded on a 1% agarose gel in 1× TAE at 100 V for 30 min at room temperature.

Atomic force microscopy (AFM)

For AFM, freshly cleaved mica discs were used as substrate for immobilizing DNA. Undamaged pBSK, obtained by purification using alkaline lysis method, was diluted to a final concentration of 1 ng/μl in a buffer containing 40 mM HEPES pH 7.0 and 5 mM $NiCl_2$. Mtb GroEL1 was added to a final concentration of 1 ng/μl in the reaction buffer. After 10 min at room temperature, 5 μl of the reaction mixture was adsorbed on mica for 5 min and washed with 200 μl of Milli-Q grade water for three times. During sample preparation, mounting of the AFM and measurements, biomolecules remain in buffer and are never dehydrated, keeping them functional. Bioscope I Atomic Force Microscope using nanoscope IV (DI, Santa Cruz) was used for imaging. All imaging was performed at room temperature with fluid tapping mode AFM. The images were analyzed using NanoScope v6 software.

Isolation of nucleoids from Mtb

A single colony of *M. tuberculosis* was inoculated in Middlebrook 7H9 medium supplemented with ADC (BD biosciences) and 0.2% Tween 80 and grown to stationary phase, subcultured and allowed to grow. One-percent Glycine was added and further incubated for 2 h at room temperature. The culture was washed thrice with PBS and then resuspended in ice-chilled acetone. The air-dried pellet was resuspended in a buffer containing 50 mM Tris–HCl (pH 8.0), 100 mM NaCl, 1 mM EDTA, 0.5% NP40, 20% sucrose, 1mg/ml of lysozyme and protease inhibitor cocktail (Roche), incubated for 2 h, pelleted at 3000 × *g* and the supernatant loaded on a 12–60% sucrose gradient. This gradient was centrifuged at 5000 rpm in a swing bucket rotor for 15 min and the bottom of the tube punctured to collect fractions. Presence of DNA in the fractions was assayed by determining the OD_{260}. The volume of the fractions corresponding to the sucrose gradient was plotted against the amount of DNA determined. The fractions with highest DNA content were considered to be fractions containing nucleoids from Mtb (18,19).

Mouse monoclonal antibody against purified Mtb GroEL1 was custom generated (Bangalore Genei). The antibody was found to be highly specific. The isolated nucleoids were assayed for the presence of Mtb GroEL1 by western Blot using the monoclonal antibody.

Chromatin immunoprecipitation (ChIP) assay and Southern blot analysis

ChIP assay was performed using Mtb H37Rv strain. Exponentially growing Mtb cells were cross-linked using 1% formaldehyde and the reaction terminated by adding 125 mM Glycine. The cells were washed thrice with PBS and resuspended in buffer containing 0.5 M sucrose, 20 mM HEPES–KOH pH 7.4, 2 mM EDTA and 7 mM β-mercaptoethanol. Protease inhibitor cocktail (Roche Diagnostics, Germany) and 0.5% NP40 were added and cells ruptured in a bead beater and centrifuged at 2000 × *g* to remove the unlyzed cells. The supernatant was sonicated in a Branson Sonifier (or Sonicator) thrice for 60 s each on ice to ensure that the fragments of size <750 bp were obtained. The supernatant was pre-cleared; anti-Mtb GroEL1 antibody added and kept overnight at 4°C. The sample was incubated with 40 μl of Protein A/G agarose beads (Santa Cruz Biotechnology, Inc) for 1 h. The pellet washed with 1 ml each of low salt wash buffer (0.1% SDS, 0.1% Triton X-100, 2 mM EDTA, 20 mM Tris–HCl pH 8.0 and 150 mM NaCl), high salt wash buffer (0.1% SDS, 0.1% Triton X-100, 2 mM EDTA, 20 mM Tris–HCl pH 8.0 and 500 mM NaCl), LiCl wash buffer (250 mM LiCl, 1% NP40, 1% deoxycholate, 1 mM EDTA, 20 mM Tris–HCl pH 8.0) and twice with TE (10 mM Tris–HCl pH 8.0, 1 mM EDTA pH 8.0) buffer, and eluted with buffer containing 10 mM Tris–HCl pH 8.0, 1 mM EDTA pH 8.0, 1% SDS and 0.1 M $NaHCO_3$. The eluate was reversed cross linked by incubating at 65°C for 6 h and adding 300 mM NaCl. An amount of 1 μg RNase A and 200 μg Proteinase K was further added and incubated for 1 h at 55°C. The DNA was purified using QIAquick PCR purification kit (Qiagen) and was labeled using Megaprime DNA-labeling systems (GE Healthcare) and αP^{32} dCTP as the labeling agent. The probe was subjected to Southern blot hybridization with ~15 μg of genomic DNA from Mtb digested with EcoRI and BamHI, the fragments resolved on a 1% agarose gel, UV cross linked and subjected to Southern blot hybridization with radiolabeled ChIP eluate. The N+ Hybond membrane were hybridized at 65°C overnight in 6× SSC, 5× Denhardt's reagent,

0.5% SDS, 1 mg/ml sheared salmon sperm DNA, 10% Dextran sulphate. The membrane was washed thrice for 30 min with 0.5× SSC and 0.5% SDS at 65°C. The membrane was wrapped and radioactive signals were read on Typhoon 9200 Phosphor imager (GE Healthcare Lifescience).

Immunofluorescence microscopy

Indirect immune-fluorescence microscopy was performed as described (20–22) with minor modifications. Mtb H37Rv cells from exponentially growing bacterial cells ($OD_{600\,nm}$ ~0.8) were smeared on slides, air dried and fixed by incubation with 3% paraformaldehyde in 1× PBS for 15 min at room temperature. The slides were then washed three times with 1× PBS and permeabilized by exposing to 2% toluene for 2 min. The slides were again washed thrice with 1× PBS; air dried, dipped in chilled methanol for 5 min and then in chilled acetone for 30 s. These slides were further washed thrice with 1× PBS and blocked with 2% BSA for 2 h at room temperature. The slides were incubated with appropriate dilution of anti-Mtb GroEL1 monoclonal antibody in 1% BSA–PBS. After extensive washing with 1× PBS, the slides were incubated with Goat anti-mouse IgG Alexa Fluor 594 conjugated secondary antibody (Invitrogen) at a dilution of 1:2000, at room temperature for 1 h. The slides were washed thrice with 1× PBS followed by addition of 10 µl of 4′,6-diamino-2-phenylindole (DAPI) (Invitrogen) in mounting media. The cells were visualized on a Leica TCS SP5 confocal microscope. In the controls for assessing specificity of the primary antibody, incubation with the primary antibody was omitted.

RESULTS

Mtb GroEL1 binds DNA with high affinity in a sequence non-specific manner

The purified recombinant Mtb GroEL1 was very homogenous, and confirmed to be a dimer as reported by us earlier (15). The GroEL1: DNA binding was accidentally discovered while studying the binding of heat shock repressor, HrcA to the conserved upstream-regulatory element, CIRCE (Controlling Inverted Repeat for Chaperone Expression). Previous experimental evidence had suggested that *Bacillus subtilis* HrcA is maintained in an active conformation that is able to bind the CIRCE sequences only in association with the GroEL chaperonin (23). We contrarily observed through electrophoretic mobility shift assays (EMSA) that the GroEL1 of Mtb, but not HrcA, binds tightly to the CIRCE2FR (TTAGCCGATTGCCATCTAGCACTCTATACATGAGAGTGCTAGCACTCAAGGGCGCCCCCT) element. This observation was further tested using biotinylated CIRCE4FR oligonucleotides coupled to streptavidin coated paramagnetic beads, to pull down GroEL1 from Mtb cell lysates. Analysis of the proteins eluted in these experiments by Mass Spectrometry confirmed the presence of Mtb GroEL1 (data not shown).

In order to test if other GroELs bound DNA similarly, we performed EMSA with Mtb GroEL-2 and GroELs from other species. In these experiments, whereas Mtb GroEL-2, *M. leprae* Cpn60.2, Human Hsp60 and *E. coli* GroEL failed to bind DNA, only non-$(His)_6$ Mtb GroEL1 exhibited DNA-binding ability under similar conditions (Figure 1A and Supplementary Figure 1). Since only Mtb GroEL1 bound DNA among the five GroELs tested, it appears that Mtb GroEL1 might have specifically acquired this property during evolution. Moreover, our result that non-$(His)_6$ GroEL1 binds DNA unlike the $(His)_6$-Mtb GroEL1 indicates that the $(His)_6$-tag at the N-terminal end interferes with the DNA-binding activity of Mtb GroEL1. The nucleotide binding by GroEL1 revealed an apparent dissociation constant (K_d) of 143 nM (Figure 1B). Thus, these observations clearly show that GroEL1 binds CIRCE DNA with a high affinity.

In order to explore the range of DNA sequences or structures that Mtb GroEL1 is able to recognize, we studied the binding of GroEL1 to different sequences. Figures 2A and B depict the binding of GroEL1 to oligonucleotides which are either annealed to their complementary strands forming a double-stranded oligonucleotide (Figure 2A), or simply the oligonucleotides without their complementary strands so that these remain single stranded or form hairpin structures wherever appropriate (Figure 2B). Moreover, as the single-stranded CIRCE2F has an intrinsic propensity to form a stem-loop like structure, we mutated the CIRCE2F sequence in order to generate different single-stranded structures. The mutated sequences were such that the loop between the inverted sequence element was deleted (MutO2), stem part on either side of the inverted repeat was replaced to disrupt the stem loop structure (MutO3 and MutO6), the flanking sequences on both the 3′ and 5′ ends were removed (MutO4), and the loop between the inverted repeat element was increased in size (MutO5). Lastly randomized sequence of CIRCE maintaining the same nucleotide composition was also tested (MutO7). A pictorial depiction of the mutated oligonucleotides and their sequences is given in Table 1. Surprisingly, GroEL1 bound to all these oligonucleotides suggesting that it might bind DNA in a sequence and structure independent manner. Furthermore, GroEL1 also interacted with nicked and fork shaped DNA structures (Supplementary Figure 2). The calculated pI of the protein was estimated to be ~4.8, and it seems unlikely that it would bind DNA due to its overall basic charge. Therefore, these experiments suggest that Mtb GroEL1 binds DNA without any sequence or structure specificity.

The non-specificity of DNA binding led us to explore the interaction of GroEL1 with a longer fragment of DNA. The longer fragment comprised the sequence corresponding to –100 to –240-nt upstream of the *groES (Rv3418c)* gene. This experiment interestingly revealed gradual appearance of slower mobility complexes with increasing concentrations of GroEL1. Moreover, as the formation of higher retarded complexes increased, the less retarded complexes gradually disappeared (Figure 2C). These results indicate multiple GroEL1 molecules binding to the longer fragment of the DNA via non-specific sequence recognition.

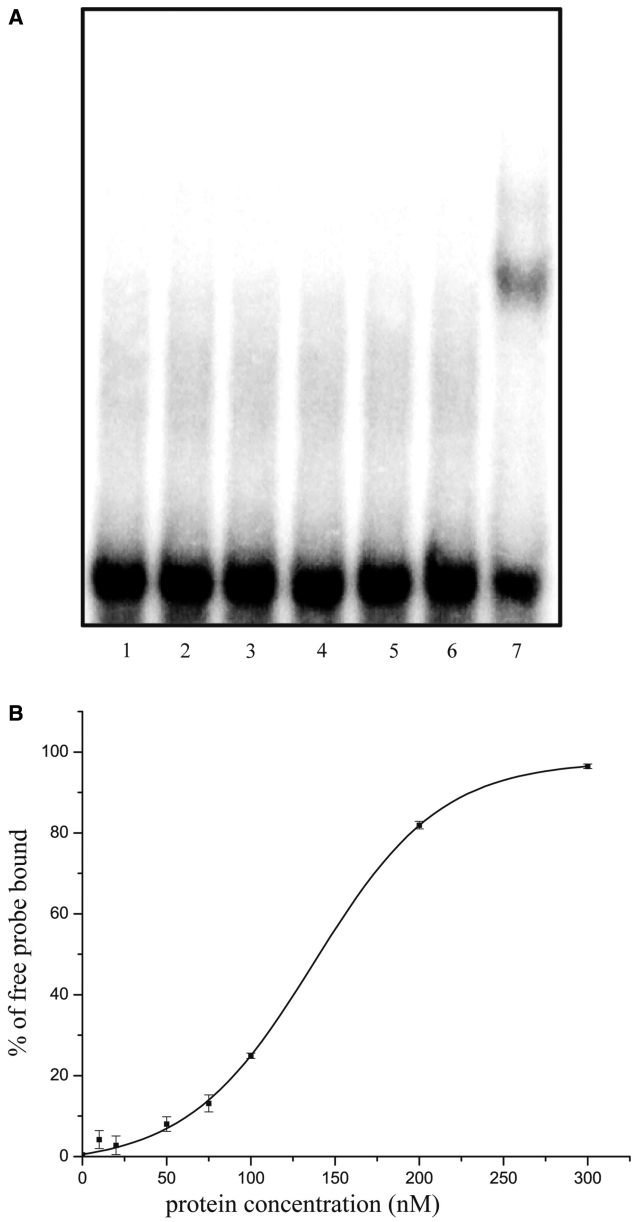

Figure 1. Binding of Mtb GroEL1 to DNA. (**A**) DNA-binding activity of GroELs from different organisms. The proteins (in 1 μM concentration) tested for DNA-binding are lanes, 1: Probe alone; 2: $(His)_6$-tagged Mtb GroEL1; 3: Mtb GroEL-2; 4: *M. leprae* Cpn60.2; 5: Human Cpn60; 6: *E. coli* GroEL; 7: Non-$(His)_6$ tagged GroEL1. ^{32}P-labeled inverted repeat DNA was used as the probe for binding assays, as chaperonin expression is known to be controlled by similar inverted repeat sequences. It is clearly seen that only non-$(His)_6$ tagged GroEL1 binds DNA, while others do not. (**B**) Determination of the binding constant between Mtb GroEL1 and DNA. The binding constants were determined by performing EMSA reactions with a 10 nM ^{32}P-labeled CIRCE2FR probe and by varying the concentrations of Mtb GroEL1 between 0–300 nM. These experiments were performed in triplicate and quantified by phosphorimager analysis. The percentage of bound probe was calculated by estimating diminishing intensity of the free probe. Binding was saturated at 300 nM concentration of the protein, which was considered to be 100% binding. The data were fitted with Sigmoidal curve, where 50% saturation corresponded to the K_d value. Error bars indicate standard error.

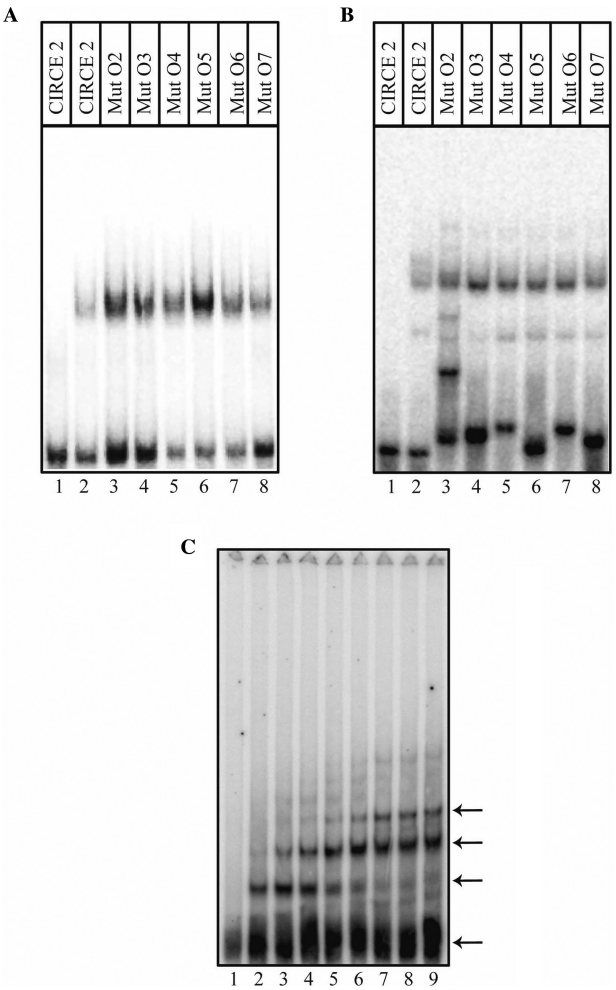

Figure 2. The binding of Mtb GroEL1 to different mutants of CIRCE2F/CIRCE2FR element. (**A**) Binding assays with annealed double-stranded oligonucleotides. The nomenclature used for different oligonucleotide probes is listed in Table 1. Lane1 shows CIRCE2FR probe alone whereas other lanes show binding of Mtb GroEL1 to Lane 2: CIRCE2FR; Lane 3: mutO2; Lane 4: mutO3; Lane 5: mutO4; Lane 6: mutO5 and Lane 7: mutO6, Lane 8: mutO7. The concentration of protein used in this experiment was 1 μM, while that of the radiolabeled oligonucleotide was 100 nM. (**B**) Binding assays with single-stranded oligonucleotides. The lane labeling is identical as in Figure 2A, except that the oligonucleotides were not annealed with their complementary strands, thus maintaining these in the single-stranded form. (**C**) Binding of different concentrations of Mtb GroEL1 to 140-bp region upstream of Mtb GroES. Lane 1, probe alone; lanes 2–9, 0.2, 0.4, 0.6, 0.8, 1, 2, 3, 4 μM of Mtb GroEL1. Appearance of more retarded bands indicates non-specific binding of Mtb GroEL1 to DNA.

GroEL1 binds preferentially to single-stranded as compared to doubled-stranded DNA

In order to further confirm if GroEL1 preferentially binds to double-stranded (dsDNA) or single-stranded DNA (ssDNA), we monitored the gel shift of radiolabeled dsDNA in the presence of increasing known concentrations of unlabeled dsDNA and ssDNA (Figure 3A). As anticipated from the results of experiments shown in Figure 2A and B, GroEL1 binds to both dsDNA and ssDNA (Figure 3B). However, we observe that ssDNA serves as a better competitor than dsDNA (Figure 3B).

Table 1. Sequences of mutated CIRCE2F oligonucleotide used in this study

CIRCE2F	TTAGCCGATTGCCATCTAGCACTCTATACATGAGAGTGCTAGCACTCAAGGGCGCCCCCT	Wild-type
MutO2	ATACTTAGCCGATTGCCATCTAGCACTCTAGAGTGCTAGCACTCAAGGGCGCCCCCTATG	no loop
MutO3	TTAGCCGATTGCCATTCCTGTACAAATACATGAGAGTGCTAGCACTCAAGGGCGCCCCCT	Stem replaced
MutO4	GTGCACTTAGCCGATTGCCATTCTATACATGAGACACTCAAGGGCGCCCCCTCTAGCTAG	Reduced stem
MutO5	TTAGCCGATTGCCATCTAGCACTCTGCGCCCCCTATACATGAGAGTGCTAGCACTCAAGG	Increased loop
MutO6	TTAGCCGATTGCCATCTAGCACTCTATACATGTTGGAACGGACACTCAAGGGCGCCCCCT	Stem replaced
MutO7	TTAGCCGATTGCCATCACGCACTACGTAGTGTCTATGTATCGATCTCAAGGGCGCCCCCT	Randomized CIRCE

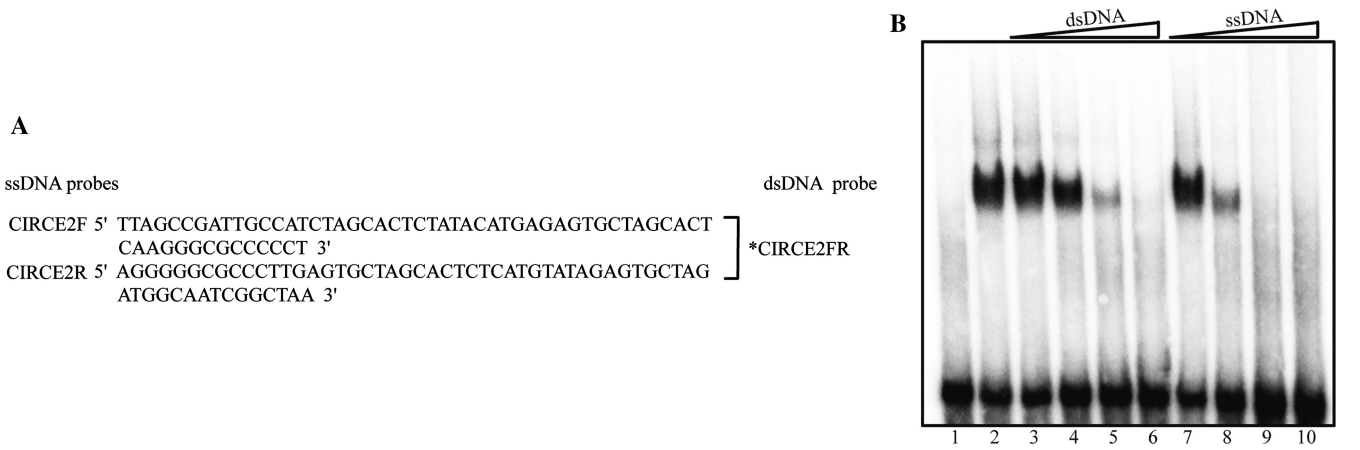

Figure 3. Mtb GroEL1 binds preferentially to single-stranded DNA. **(A)** Sequences of oligonucleotides used for performing EMSA with increasing concentration of Mtb GroEL1 using 5′ end-labeled DNA. (**B**) The comparison of the binding of dsDNA and ssDNA was studied using radiolabeled dsDNA as probe and 1×, 20×, 100×, 500× Molar excess dsDNA (unlabeled) and ssDNA (unlabeled) as competitor to radiolabeled probe. Lane 1: probe alone, lane 2: probe and 1μM GroEL, lane 3: probe and 1× dsDNA (unlabeled), lane 4: probe and 20× dsDNA (unlabeled), lane 5: probe and 100× dsDNA (unlabeled), lane 6: probe and 500× dsDNA (unlabeled), lane 7: probe and 1× ssDNA (unlabeled), Lane 8: probe and 20× ssDNA (unlabeled), Lane 9: probe and 100× dsDNA (unlabeled), Lane 10: probe and 500× dsDNA (unlabeled).

GroEL1 thus binds both ssDNA and dsDNA, but has a preference of binding ssDNA over dsDNA. Furthermore, RNA binding was tested with the RNA sequence of CIRCE, a 28-mer (UUCUUGCACUCGGCAUAGGC GAGUGCUA). It was selected to be a complementary probe to the DNA sequence tested. These experiments revealed that GroEL1 also bound RNA, but with a lower affinity than DNA (Figure 4).

GroEL1 binds to the minor groove of DNA

In order to test the groove specificity of binding, drugs that specifically interact with the major or minor groove of DNA were evaluated for their ability to compete with DNA binding. There was no formation of the GroEL1: DNA complex in the presence of Actinomycin D, a minor groove-binding drug (Figure 5A). On the other hand, increasing concentrations of Methyl green, a major groove binder did not affect the formation of GroEL1: DNA complex (Figure 5B). The ability of Actinomycin D to compete with GroEL1: DNA complex formation clearly demonstrates that GroEL1 binds to DNA through the minor groove. The minor-groove-binding proteins are typically known to bind DNA with high affinity, exhibit very different global folds and also remodel the DNA conformation in distinct ways (24). It was therefore tempting to explore the role of GroEL1 in maintaining DNA conformation.

GroEL1 condenses naked DNA into globular structures

Sequence non-specificity of DNA recognition by GroEL1 suggested that GroEL1 might be involved in the protection of DNA against external damage. We studied the protection of DNA from external damage by two different experiments, firstly, we tested the prevention of formation of nick by Mtb GroEL-1 in supercoiled DNA in the presence of oxidative radicals and secondly, tests were performed to study the protection of DNA from DNaseI digestion. In our experiments, Mtb GroEL1 was seen to

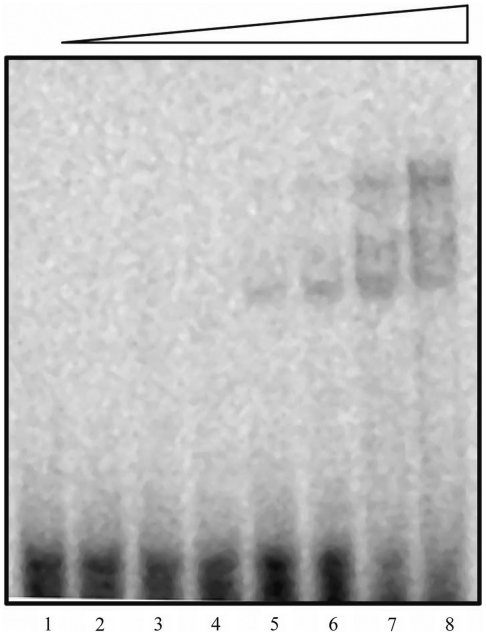

Figure 4. Binding of Mtb GroEL1 to γP^{32} labeled RNA. The binding of different concentration of Mtb GroEL1 to γP^{32}-labeled RNA sequence (UUCUUGCACUCGGCAUAGGCGAGUGCUA)—lane 1, probe alone, lanes 2–8, 0.25, 0.5, 0.75, 1, 2, 3, 4 μM of Mtb GroEL1. The concentration of γP^{32}-labeled probe used in all the lanes was 4 nM.

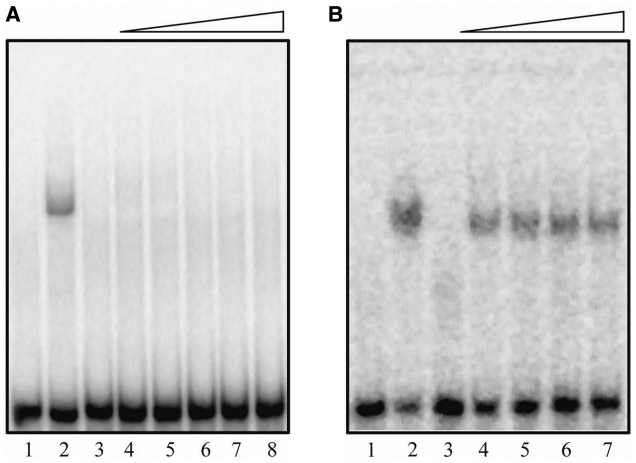

Figure 5. Mtb GroEL1 interacts with DNA through the minor grove. (**A**) CIRCE2FR oligonucleotide was annealed with its complementary strand to form dsDNA which was then radiolabeled with γP^{32} ATP. The probe was incubated with increasing concentration of Actinomycin D, a minor groove binder (lanes 4–8, 0.1 mM–1 mM). The reactions were further incubated with 1 μM GroEL1 and resolved on native PAGE. As controls, labeled DNA was either loaded alone (lane 1), with GroEL1 (lane 2) or with 1 mM Actinomycin D (lane 3). (**B**) As in panel A, DNA was annealed with its complementary strand to form dsDNA and radiolabeled with γP^{32} ATP. The probe was incubated with increasing concentration of Methyl Green, a major groove binder (lanes 4–7, 0.1–0.5 mM). The reactions were further incubated with 1 μM GroEL1 and resolved on native PAGE. As controls, labeled DNA was either loaded alone (lane 1), with GroEL1 (lane 2) or with 0.5 mM Methyl Green (lane 3).

protect supercoiled DNA from damage by hydroxyl radicals generated by the metal catalyzed oxidation system (Figure 6A). GroEL1 was also observed to protect supercoiled plasmid, pBluescript II SK (+), against DNase I digestion (Figure 6B). Thus, these findings suggest that, the non-specific binding to DNA indeed allows GroEL1 to protect DNA against extrinsic damage.

The nature of complexes formed by GroEL1 and DNA were further examined by AFM. AFM images of 2958-bp supercoiled pBluescript II plasmid DNA in absence of GroEL1 showed uniform structures (Figure 6C), whereas GroEL1 alone was globular (Figure 6D). Many of the GroEL molecules appeared as doublets (Figure 6D), reinforcing our earlier observations that the recombinant GroEL1 is dimeric (15). Interestingly, the protein–DNA complexes showed different degrees of condensation ranging from partial condensation to very condense globular structures (Figure 6E). This condensation of extended, unconstrained DNA molecules into globular particles is comparable with coil-globule transitions induced by neutral polymers. Therefore, the AFM images clearly establish that GroEL1 is capable of condensing a large DNA.

Evidence for *in vivo* DNA binding and possible functional significance

The *in vitro* observations of GroEL1 in protection of DNA against extrinsic damage and condensation of plasmids are reminiscent of NAP. We therefore examined the presence of *E. coli* NAP protein homologs in Mtb (Table 2). Extensive sequence based searches in the Mtb genome using a core set of 10–20 NAP of *E. coli* revealed the presence of only HU, CbpA and IciA in Mtb (Table 2). Other proteins, namely Dps, Hfq, H-NS and StpA were conspicuous by their absence in the Mtb genome as indicated by their low BLAST scores. Similarly, among the five sequence-specific NAP CbpB, DnaA, Fis, IHF and Lrp, homologs of only DnaA, Lrp and IHF appear to be present in the Mtb genome. Interestingly Dps, which has the function of protecting DNA under starvation conditions in *M. smegmatis*, was reported to be absent in the Mtb genome (25). Thus, in the apparent absence of a number of NAP and the ability of Mtb GroEL1 to DNA, a possibility arises that Mtb GroEL1 might have adopted nucleoid association function via non-specific DNA binding.

We sought to test the hypothesis that Mtb GroEL1 might be associated with the nucleoid structures by isolating Mtb nucleoids using sucrose gradient centrifugation as described in 'Materials and methods' section (Figure 7A). The presence of GroEL1 in the purified nucleoids was confirmed by SDS–PAGE followed by western blot analysis using anti-GroEL1 mouse monoclonal antibody (Figure 7B and C). As a control, presence of two cytosolic proteins, GroEL-2 and AhpC, was tested in the purified nucleoids by western blotting. However, these were not detected. It is possible that the presence of GroEL1 in the nucleoids is spurious. Alternately, its presence in the nucleoids could be because of its ability to bind to chromosomal DNA. To distinguish between the two possibilities we performed ChIP analysis on the Mtb nucleoids. Formaldehyde cross-linked DNA–protein complex within

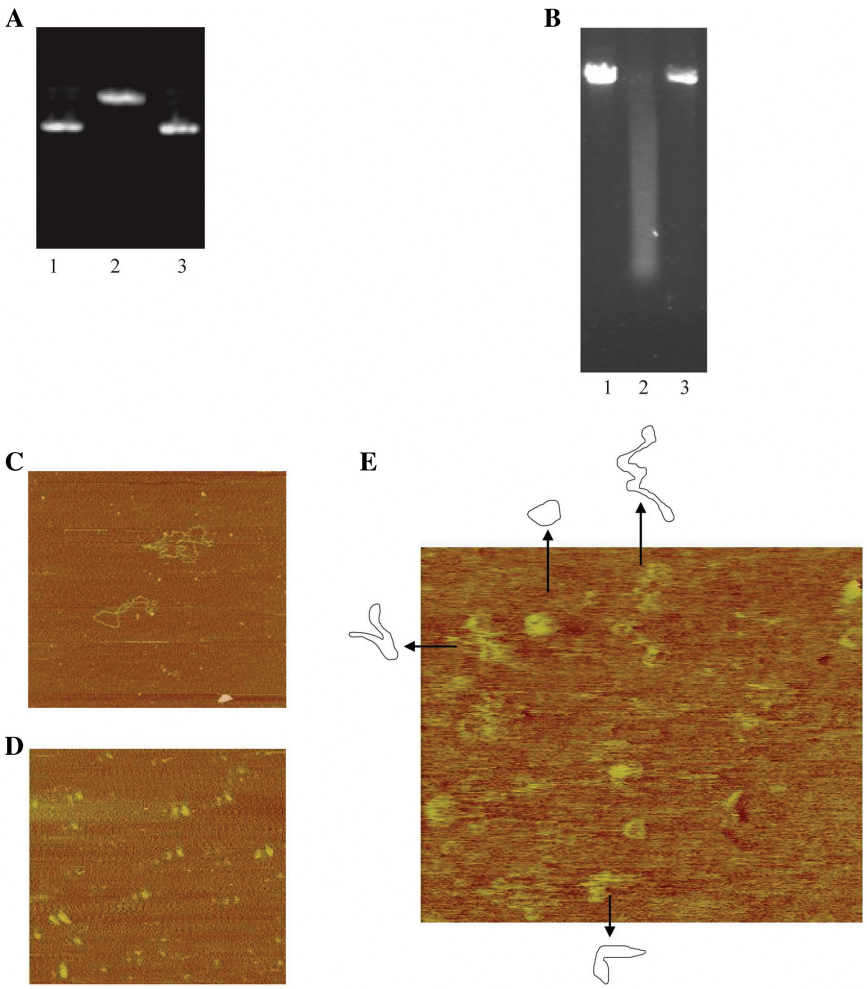

Figure 6. Mtb GroEL1 protects plasmid DNA from DNase I digestion and oxidative radicals, and condenses DNA as evidenced by AFM. (**A**) Protection of plasmid supercoiling from oxidative damage: 0.8% Agarose gel scan shows two forms of plasmid DNA (pBSK) bands. Lane 1 shows 200 ng plasmid DNA without metal-catalyzed oxidation (MCO) system, lane 2 shows plasmid DNA with MCO system and lane 3 shows plasmid DNA preincubated with 14 μM Mtb GroEL1 with MCO system. (**B**) Protection of pBSK against DNase I digestion: lane 1 pBSK without DNase I, lane 2: pBSK digested with DNase I, and lane 3: pBSK incubated with GroEL1 prior to digestion with DNase I. 75 ng of pBSK and 7 μM Mtb GroEL1 was used in the assay. **(C)–(E)** AFM showing Mtb GroEL1 mediated DNA condensation. (C) pBSK DNA, scan size is 3 μm, (D) 1 ng/μl solution of pure Mtb GroEL1, scan size is 1.2 μm and (E) plasmid pBSK and Mtb GroEL1 incubated together for 10 min at room temperature, scan size is 586.5 μm. As is clearly seen, Mtb GroEL1 has profound effect on condensing the plasmid DNA.

the Mtb nucleoids were subjected to immunoprecipitation using GroEL1-specific antibody. The immunoprecipitated DNA was used as a probe in a Southern hybridization experiment where Mtb genomic DNA digested with different restriction enzymes was blotted on a Nylon membrane (see 'Materials and methods' section). As can be seen from Figure 7D, anti-GroEL1 immunoprecipitated fraction, when radiolabeled and used as a probe, binds to several fragments of the Mtb genomic DNA. Even though the pattern of hybridization appears as a smear indicating non-specific binding of GroEL1 to the Mtb chromosomal DNA, a few intensely stained bands can also be seen. This suggests that although GroEL1 binds DNA non-specifically, it might bind some DNA sequences with a higher affinity. In a similar ChIP experiment, anti-GroEL-2 antibody did not show binding to chromosomal DNA. No DNA was observed when the GroEL-2 bound fraction was electrophoresed on an agarose gel or by measuring its Optical Density at 260 nm (data not shown). Therefore, the observed presence of GroEL1 in the Mtb nucleoids is a consequence of its ability to bind Mtb chromosomal DNA.

To further determine if the nucleoid association of Mtb GroEL1 is also observed *in vivo*, Mtb cells were visualized by immunofluorescence using confocal microscopy (Figure 8). Mouse monoclonal antibody against GroEL1 labeled with Alexa-fluor 594 colocalized with the nucleoid DNA stained with DAPI (Figure 8; panel GroEL1 AF594 + DAPI). However, GroEL1 was not found to be colocalized over the entire length of the DNA, but rather in distinct areas, confirming our ChIP–Southern results that there might be regions of Mtb DNA which have higher affinity for GroEL1. These results therefore confirmed that Mtb GroEL1 indeed is a NAP.

DISCUSSION

Prokaryotic GroEL chaperonins are known to facilitate *de novo* folding of 10–15% cytosolic proteins (26,27). The universality of GroEL mechanism and the occurrence of *groES* and *groEL* genes in all organisms are suggestive of the criticality of *groEL* in all life forms. The chaperonin genes in many prokaryotic species, such as Mycobacteria, have been observed to be duplicated, possibly to provide these organisms with adequate redundancy in the protein folding apparatus (16). Intriguingly, some of the paralogous *groEL* genes do not appear to promote refolding of model substrates *in vitro* (15), or *in vivo* as evidenced by lack of functional complementation in the *E. coli groEL* Ts allele (28), (Kumar *et al.*, personal communication). Thus, the role of *groEL* duplication in these organisms is not clearly understood.

Gene duplication is an important evolutionary force that provides an organism an opportunity to evolve new functions (29). Gene duplication events in evolution have been suggested to impart selective advantage to organisms by offering differentiated gene regulation or degeneracy of function. Gene duplication has also been suggested to lead to evolution of promiscuous functions, where this serves as a mechanism to acquire varied substrate spectrum (30).

Table 2. Comparison of NAPs in Mtb and *E. coli*

S/No.	*E. coli*	*M. tuberculosis*	*e*-value	Remarks
1	HNS	Rv2477c	7.2	Absent
2	Hfq	Rv0511	0.55	Absent
3	StpA	Rv3296	1.4	Absent
4	Dps	Rv1522c	0.14	Absent
5	HupA	Rv2986 (HupB)	$8e^{-}$	Best BLAST hits for all the three proteins of *E. coli* correspond to the same ORF in Mtb.
6	HupB	Rv2986 (HupB)	$4e^{-11}$	
7	IHF-A	Rv2986 (HupB)	$3e^{-14}$	
8	IHF-B	Rv2986	0.97	Absent
9	CbpA	Rv0352 (DnaJ1) Rv2373c (DnaJ2)	$8e^{-40}$ $8e^{-22}$	Best BLAST hit corresponds to the same ORF
10	Fis	Rv3077	1.3	Absent
11	Lrp	Rv3219c	$3e^{-17}$	Present

The *e*-values of BLAST scores, when *E. coli* protein sequences are searched in the *M. tuberculosis* genome, are shown. The 11 proteins known to be involved in nucleoid association in *E. coli* were chosen from literature (2).

Such functional variations obtained as a result of gene duplication provide organisms an adaptive advantage and a better chance of survival. One of the possibilities of *groEL* paralogy in few prokaryotes might therefore be evolution of promiscuous biochemical functions.

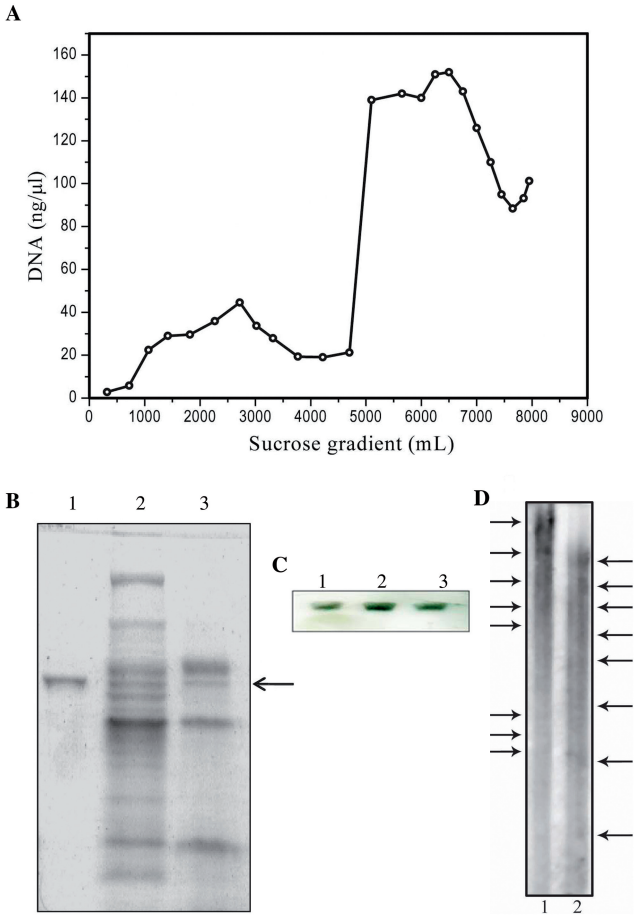

Figure 7. *In vivo* evidence for the Mtb GroEL1 binding to DNA. (**A**) Isolation of nucleoid from *M. tuberculosis H37Rv* strain by sucrose gradient centrifugation. (**B**) The isolated nucleoids separated on a 10% SDS–PAGE (lane 3) along with Mtb whole cell lysate (lane 2) and purified Mtb GroEL1. (**C**) The presence of Mtb GroEL1 in nucleoids is confirmed by western blotting (lane 2) along with Mtb whole cell lysate (lane 1) and purified Mtb GroEL1 (lane 3) as control. (**D**) Southern blot hybridization with restriction enzyme digested genomic DNA of Mtb and ChIP eluted DNA as probe. Lane 1: EcoRI digested Mtb genomic DNA, lane 2: BamHI digested Mtb genomic DNA.

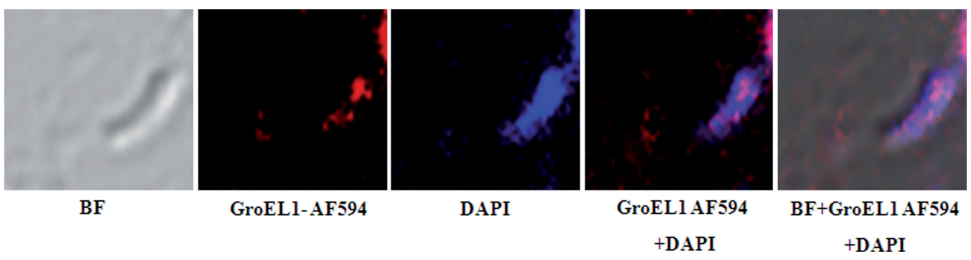

Figure 8. Mtb GroEL1 is associated with the nucleoid of Mtb. Brightfield image of Mtb H37Rv is shown. Cells were stained with DAPI to visualize the nucleoid (blue) and Alexa fluor 594 conjugated secondary antibodies against Mtb GroEL1 monoclonal antibody (red) to visualize Mtb GroEL1. The superimposition of DAPI stained nucleoid and Alexa fluor 594 stained Mtb GroEL is shown. The pink color clearly indicates the colocalization of GroEL1 with Mtb nucleoids.

Mtb GroELs have earlier been reported to exist in unusual oligomeric state with a weak chaperonin activity (15). The C-terminal of GroEL1 is rich in histidine residues, which has been reported to be important for biofilm formation in *M. smegmatis* (31). Moreover, Mtb lacking GroEL1 is shown to be defective in granuloma formation (32). Although the Mtb *groEL1* mutant has no phenotype in response to addition of H_2O_2, and that our work shows that GroEL1 protects against oxidative damage, it is likely that other antioxidant proteins such as thioredoxins (33) or AhpC (34) might help protection *in vivo* by free radical scavenging. It is interesting to note that DPS and IHF proteins, which offer protection to DNA against free radicals, are present in the closely related *M. smegmatis* but yet absent in *M. tuberculosis*. The significance of the absence of these proteins in *M. tuberculosis*, and whether GroEL might perform their function of DNA protection in *M. tuberculosis* is not clear. Furthermore, the apparent K_d values obtained is comparable to that obtained for other nucleoid-associated DNA-binding proteins. Our observations therefore suggest that the modes of action of Mtb GroEL1 might be similar to the well-studied NAP.

Consistent with the above hypothesis, Mtb GroEL1 has been observed to bind to both ssDNA and dsDNA in an analogous manner as bovine zeta crystalline, ZTA1, which also binds ssDNA as well as dsDNA and has roles in gene expression, growth and differentiation of bovine lens (35). This hypothesis is further supported by the fact that GroEL1 binds DNA through its minor groove which is typically considered to be insufficient for specific recognition. Many of the minor groove-binding proteins usually bend DNA and recruit other proteins through their interactions with hydrophobic patches to effectively act as a DNA chaperone. Mtb GroEL1 therefore might perform similar functions, namely, to compact the chromosomal DNA via minor groove and sequence independent binding, and by recruiting other proteins through its hydrophobic patches.

We hypothesize that Mtb GroEL1 might have changed substrate specificity from polypeptides to polynucleotides via the *E. coli* GroEL-like substrate-recognizing apical domain. Our earlier observations that Mtb GroEL1 exists as a dimer, and not as a tetradecamer, lead us to speculate that subtle mutations are responsible for a change in the oligomeric state of the protein and thereby substrate specificity. It is therefore tempting to suggest that evolutionary tinkering has led to Mtb GroEL1 acquiring the property of nonspecific DNA binding and an ability to act as a DNA chaperone.

SUPPLEMENTARY DATA

Supplementary Data are available at NAR Online.

ACKNOWLEDGEMENTS

We thank The Centre for Genomic Applications, New Delhi for assistance in MALDI TOF experiments and members of Khosla lab for help in EMSA experiments. We thank Dr Sanjeev Kapoor and the imaging facility at the Department of Plant Molecular Biology, University of Delhi, South Campus. We also thank C.M. Santosh Kumar, Ranjan Sen and Abhijit Sardesai for many useful discussions.

FUNDING

Department of Biotechnology, India; Wellcome Trust, UK; Council for Scientific and Industrial Research Senior Research Fellowships (to D.B. and G.K.); Wellcome Trust International Senior Research Fellowship (to S.C.M.). Funding for open access charge: Wellcome Trust grant WT070006MA.

Conflict of interest statement. None declared.

REFERENCES

1. Azam,T.A., Iwata,A., Nishimura,A., Ueda,S. and Ishihama,A. (1999) Growth phase-dependent variation in protein composition of the *Escherichia coli* nucleoid. *J. Bacteriol.*, **181**, 6361–6370.
2. Azam,T.A. and Ishihama,A. (1999) Twelve species of the nucleoid-associated protein from *Escherichia coli*. Sequence recognition specificity and DNA binding affinity. *J. Biol. Chem.*, **274**, 33105–33113.
3. Almiron,M., Link,A.J., Furlong,D. and Kolter,R. (1992) A novel DNA-binding protein with regulatory and protective roles in starved *Escherichia coli*. *Genes Dev.*, **6**, 2646–2654.
4. Rouviere-Yaniv,J. and Gros,F. (1975) Characterization of a novel, low-molecular-weight DNA-binding protein from *Escherichia coli*. *Proc. Natl Acad. Sci. USA*, **72**, 3428–3432.
5. Drlica,K. and Rouviere-Yaniv,J. (1987) Histone-like proteins of bacteria. *Microbiol. Rev.*, **51**, 301–319.
6. Dame,R.T. (2005) The role of nucleoid-associated proteins in the organization and compaction of bacterial chromatin. *Mol. Microbiol.*, **56**, 858–870.
7. Rimsky,S., Zuber,F., Buckle,M. and Buc,H. (2001) A molecular mechanism for the repression of transcription by the H-NS protein. *Mol. Microbiol.*, **42**, 1311–1323.
8. Dorman,C.J. (2004) H-NS: a universal regulator for a dynamic genome. *Nat. Rev. Microbiol.*, **2**, 391–400.
9. Hommais,F., Krin,E., Laurent-Winter,C., Soutourina,O., Malpertuy,A., Le Caer,J.P., Danchin,A. and Bertin,P. (2001) Large-scale monitoring of pleiotropic regulation of gene expression by the prokaryotic nucleoid-associated protein, H-NS. *Mol. Microbiol.*, **40**, 20–36.
10. Lucchini,S., Rowley,G., Goldberg,M.D., Hurd,D., Harrison,M. and Hinton,J.C. (2006) H-NS mediates the silencing of laterally acquired genes in bacteria. *PLoS Pathog.*, **2**, e81.
11. Rouviere-Yaniv,J., Yaniv,M. and Germond,J.E. (1979) *E. coli* DNA binding protein HU forms nucleosomelike structure with circular double-stranded DNA. *Cell*, **17**, 265–274.
12. Kamashev,D., Balandina,A., Mazur,A.K., Arimondo,P.B. and Rouviere-Yaniv,J. (2008) HU binds and folds single-stranded DNA. *Nucleic Acids Res.*, **36**, 1026–1036.
13. Kamashev,D. and Rouviere-Yaniv,J. (2000) The histone-like protein HU binds specifically to DNA recombination and repair intermediates. *EMBO J.*, **19**, 6527–6535.
14. Dame,R.T. and Goosen,N. (2002) HU: promoting or counteracting DNA compaction? *FEBS Lett.*, **529**, 151–156.
15. Qamra,R., Srinivas,V. and Mande,S.C. (2004) *Mycobacterium tuberculosis* GroEL homologues unusually exist as lower oligomers and retain the ability to suppress aggregation of substrate proteins. *J. Mol. Biol.*, **342**, 605–617.
16. Goyal,K., Qamra,R. and Mande,S.C. (2006) Multiple gene duplication and rapid evolution in the *groEL* gene: functional implications. *J. Mol. Evol.*, **63**, 781–787.
17. Frenkiel-Krispin,D., Levin-Zaidman,S., Shimoni,E., Wolf,S.G., Wachtel,E.J., Arad,T., Finkel,S.E., Kolter,R. and Minsky,A. (2001)

Regulated phase transitions of bacterial chromatin: a non-enzymatic pathway for generic DNA protection. *EMBO J.*, **20**, 1184–1191.
18. Miyakawa,I., Sando,N., Kawano,S., Nakamura,S. and Kuroiwa,T. (1987) Isolation of morphologically intact mitochondrial nucleoids from the yeast, *Saccharomyces cerevisiae*. *J. Cell Sci.*, **88** (Pt 4), 431–439.
19. Murphy,L.D. and Zimmerman,S.B. (1997) Isolation and characterization of spermidine nucleoids from *Escherichia coli*. *J. Struct. Biol.*, **119**, 321–335.
20. Dasgupta,A., Datta,P., Kundu,M. and Basu,J. (2006) The serine/threonine kinase PknB of *Mycobacterium tuberculosis* phosphorylates PBPA, a penicillin-binding protein required for cell division. *Microbiology*, **152**, 493–504.
21. Mukherjee,A., DiMario,P.J. and Grove,A. (2009) *Mycobacterium smegmatis* histone-like protein Hlp is nucleoid associated. *FEMS Microbiol. Lett.*, **291**, 232–240.
22. Cimino,M., Alamo,L. and Salazar,L. (2006) Permeabilization of the mycobacterial envelope for protein cytolocalization studies by immunofluorescence microscopy. *BMC Microbiol.*, **6**, 35.
23. Mogk,A., Homuth,G., Scholz,C., Kim,L., Schmid,F.X. and Schumann,W. (1997) The GroE chaperonin machine is a major modulator of the CIRCE heat shock regulon of *Bacillus subtilis*. *EMBO J.*, **16**, 4579–4590.
24. Bewley,C.A., Gronenborn,M. and Clore,G.M. (1998) Minor groove-binding architectural proteins: structure, function, and DNA recognition. *Annu. Rev. Biophys. Biomol. Struct.*, **27**, 105–131.
25. Gupta,S., Pandit,S.B., Srinivasan,N. and Chatterji,D. (2002) Proteomics analysis of carbon-starved *Mycobacterium smegmatis*: induction of Dps-like protein. *Protein Eng.*, **6**, 503–512.
26. Ewalt,K.L., Hendrick,J.P., Houry,W.A. and Hartl,F.U. (1997) In vivo observation of polypeptide flux through the bacterial chaperonin system. *Cell*, **90**, 491–500.
27. Houry,W.A., Frishman,D., Eckerskorn,C., Lottspeich,F. and Hartl,F.U. (1999) Identification of in vivo substrates of the chaperonin GroEL. *Nature*, **402**, 147–154.
28. Karunakaran,K.P., Noguchi,Y., Read,T.D., Cherkasov,A., Kwee,J., Shen,C., Nelson,C.C. and Brunham,R.C. (2003) Molecular analysis of the multiple GroEL proteins of Chlamydiae. *J. Bacteriol.*, **185**, 1958–1966.
29. Ohno,S. (1973) Ancient linkage groups and frozen accidents. *Nature*, **244**, 259–262.
30. Eason,D.D., Cannon,J.P., Haire,R.N., Rast,J.P., Ostrov,D.A. and Litman,G.W. (2004) Mechanisms of antigen receptor evolution. *Semin. Immunol.*, **16**, 215–226.
31. Ojha,A., Anand,M., Bhatt,A., Kremer,L., Jacobs,W.R. Jr. and Hatfull,G.F. (2005) GroEL1: a dedicated chaperone involved in mycolic acid biosynthesis during biofilm formation in mycobacteria. *Cell*, **123**, 861–873.
32. Hu,Y., Henderson,B., Lund,P.A., Tormay,P., Ahmed,M.T., Gurcha,S.S., Besra,G.S. and Coates,A.R. (2008) A *Mycobacterium tuberculosis* mutant lacking the groEL homologue cpn60.1 is viable but fails to induce an inflammatory response in animal models of infection. *Infect. Immun.*, **76**, 1535–1546.
33. Akif,M., Khare,G., Tyagi,A.K., Mande,S.C. and Sardesai,A.A. (2008) Functional studies of multiple thioredoxins from *Mycobacterium tuberculosis*. *J. Bacteriol.*, **190**, 7087–7095.
34. Chauhan,R. and Mande,S.C. (2002) Site-directed mutagenesis reveals a novel catalytic mechanism of *Mycobacterium tuberculosis* alkylhydroperoxidase C. *Biochem. J.*, **367**, 255–261.
35. Kranthi,B.V., Balasubramanian,N. and Rangarajan,P.N. (2006) Isolation of a single-stranded DNA-binding protein from the methylotrophic yeast, *Pichia pastoris* and its identification as zeta crystallin. *Nucleic Acids Res.*, **34**, 4060–4068.